Heliyon 9 (2023) e21826

Contents lists available at ScienceDirect

Heliyon

journal homepage: www.cell.com/heliyon

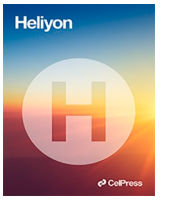

Multi-component analyses of raspberry: Optimization of extraction procedure and network pharmacology

Xuming Chen, Xiaochun Shi, Xiaohong Li *

School of Pharmaceutical Sciences, Zhejiang Chinese Medical University, Hangzhou, Zhejiang, China

ARTICLE INFO

Keywords:
Raspberry
Factorial test
Analysis of variance
Ant colony neural network
Optimization of extraction procedure

ABSTRACT

The contents of ellagic acid and kaempferol-3-*O*-rutinoside, the chief active components of raspberry, are considered the quality control indices of raspberry. This work employed the ant colony neural network (ACO-BPNN) to optimize their extraction processes, and the combination of network pharmacology and molecular docking technology to unveil the potential pharmacological effects of these components. Based on the single-factor test (ultrasonic time, ethanol concentration, ultrasonic temperature, and solid-liquid ratio), a factorial experiment with 4-factors and 3-levels was conducted in parallel for 3 times. The multi-factor analysis of variance results revealed high-order interactions among the factors. Then, the ACO-BPNN model was established to characterize the complex relationship of experimental data. After further verification, relative errors were all less than 8 %, implying the model's effectiveness and reliability. Moreover, with the network pharmacology, 66 key targets were screened out and mainly concentrated in PI3K-AKT, MAPK, and Ras signal pathways. Molecular docking revealed the binding sites between active components and key targets.

1. Introduction

Raspberry is the edible fruit of Rubus chingii Hu (Rosaceae) [1]. This plant species is mainly distributed in Guangxi, Jiangxi, Zhejiang, and Fujian provinces of East China. Raspberry is also a medicinal fruit that is sweet, sour, and warm. The raspberry fruit has a reputation as a "golden fruit." It exhibits pharmacological effects such as antioxidation, antitumor, and blood sugar- and blood lipid-lowering effects and can be used clinically to treat enuresis due to kidney deficiency, frequent urination, impotence, premature ejaculation, and spermatorrhea [2,3]. It is known for nourishing the liver and kidneys, improving eyesight, and blackening hair. R. palmatum has been included in Chinese Pharmacopoeia for its medicinal benefits [4–6]. The main active components of raspberry fruit are tannins, terpenoids, and flavonoids. Ellagic acid ($C_{14}H_6O_8$) is the main component of tannins and has several bioactive functions, such as antioxidant, anticancer, antimutation effects, and inhibition of the human immunodeficiency virus [7]. Kaempferol-3-*O*-rutinoside ($C_{27}H_{30}O_{15}$) is the main component of flavonoids and exhibits anti-hepatotoxic, antioxidation, antiaging, and neuroprotective effects [8]. In the 2020 edition of Chinese Pharmacopoeia, the contents of ellagic acid and kaempferol-3-*O*-rutinoside were considered quality control indices for raspberry and the respective extraction conditions and methods for these two components have been discussed. However, research on optimizing the extraction conditions of the two components is limited.

TCM has very complex chemical components, and the relationship between the extraction conditions and the yield is quite

* Corresponding author. Baichuan Street 260, Hangzhou, Zhejiang, 311402, China.
E-mail address: li_xiaoh2005@163.com (X. Li).

https://doi.org/10.1016/j.heliyon.2023.e21826
Received 14 March 2023; Received in revised form 28 October 2023; Accepted 30 October 2023
Available online 4 November 2023

intricate. Thus, it is necessary to establish a new technology that can quantitatively describe the relationship between conditions and yield. In this study, the quality markers of raspberry, ellagic acid, and kaempferol-3-*O*-rutinoside, were used as extracts. On the basis of the single-factor test, the main factors affecting the yield of the two components and the level of each factor were determined. In order to obtain accurate and reliable optimum extraction conditions, the factorial test results were analyzed by multi-factor analysis of variance to explore the interaction among four experimental factors, and based on this conclusion, ACO-BPNN was established. More specifically, using the global optimization function of the ant colony algorithm, the parameters in the model are optimized, and using the neural network model, the best extraction process is determined. ACO-BPNN was used to optimize the conditions of the two components individually extracted from raspberry and their combined extraction, which thus formed the foundation and provided a reference for further studying the material basis of raspberry efficacy, thereby ensuring the quality control of raspberry. The flow chart in Fig. 1 shows the continuity of two research tasks: extraction experiment and intelligent algorithm.

Network pharmacology integrates new disciplines such as bioinformatics and network science. It can establish the molecular association network between drugs and diseases from the system level and biological network, revealing the pharmacological mechanism of drugs as a whole [9]. Therefore, network pharmacology is a crucial technique for developing innovative drugs and significantly contributes to the development of a new research model of "multi-component, multi-target, and multi-way" in TCM [10]. However, reports on the network pharmacology of the main raspberry components are few. Hence, in this study, the main targets and pathways of ellagic acid and kaempferol-3-*O*-rutinoside in raspberry were discussed using network pharmacology in combination with molecular docking technology. The study findings act as a reference for optimization of extraction procedure and further research on the pharmacological mechanism of raspberry. The flow chart in Fig. 1 shows the correlation between the optimization of extraction procedure and network pharmacology research.

2. Materials and methods

2.1. Reagents and feedstock

Ultra-pure water was prepared through the Millipore water-purification system (Millipore Co., Ltd., Billerica, MA, USA). Ethanol (Batch No: 2014090901) was purchased from Kelon Chemical Reagent Factory (China) and phosphoric acid (Batch No: AT20100318) was purchased from Sinopharm Chemical Reagent Co., Ltd. (China). Acetonitrile (Batch No: AS1122-801) and methanol (chromatographically pure, MS1922-801) were purchased from Tiandi Co., Ltd. (USA). Kaempferol-3-*O*-rutinoside (Batch No: PS0833-0025) was purchased from Pusi Biotechnology Co., Ltd. (Chengdu, Sichuan). Ellagic acid (Batch No: CDAA-280576) was purchased from Yancheng Technology Co., Ltd. (Beijing, China). The purity of Kaempferol-3-*O*-rutinoside and Ellagic acid was ≥98 %. Experimental raspberry slices were purchased from Chinese Herbal Pieces Co., Ltd. of the Zhejiang Chinese Medical University as were the dried fruits of Rubus chingii Hu.

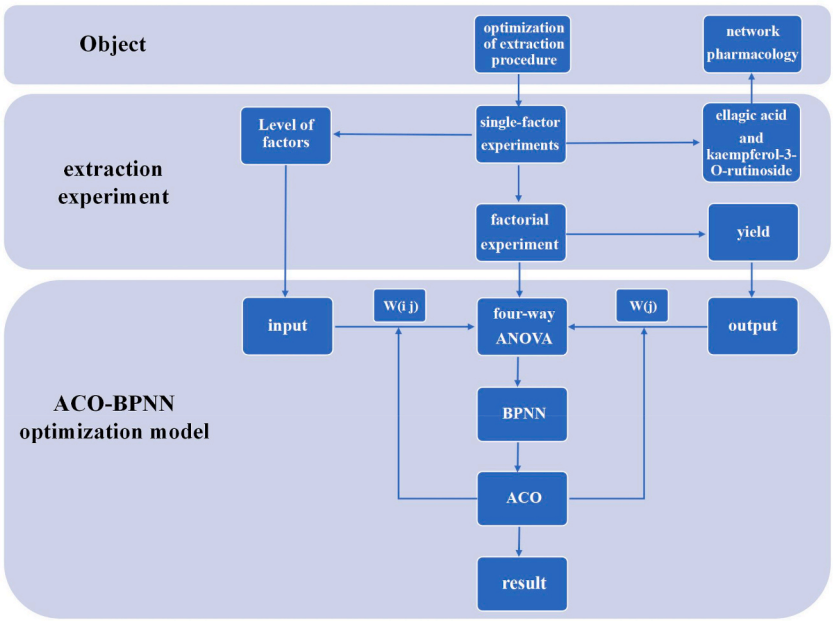

Fig. 1. Flow chart of optimization of extraction procedure and network pharmacology.

2.2. Preparation of sample and standard solutions

Raspberry powder (~5.00 g) was accurately weighed and 100 mL of 70 % ethanol was added before ultrasonic treatment at 50 °C for 30 min, cooling to room temperature, shaken well, and centrifuged. The supernatant was collected and filtered through a 0.22 μm microporous membrane for HPLC analysis.

Moderate kaempferol-3-*O*-rutinoside and ellagic acid were precisely weighed and dissolved in chromatography-grade methanol to prepare the mixed standard solution for HPLC analysis. The concentrations of kaempferol-3-*O*-rutinoside and ellagic acid were 130.0 μg/mL and 280.0 μg/mL, respectively.

2.3. Chromatographic method

The following chromatographic conditions were employed: chromatographic column: EclipseXD-C18 column (250 × 4.6 mm, 5 μm); Mobile phase: 0.2 % phosphoric acid water (A) - acetonitrile (B), gradient elution (0–6 min, 5–20 % B; 6–25 min , 20–35 % B); Detection wavelength: 350 nm; Column temperature: 30 °C; Flow rate: 1.0 mL/min; The injection volume: 10 μL.

2.4. Method validation

2.4.1. Investigation of the linear range

The stock standard solution was diluted with methanol to prepare seven mixed standard solutions of different concentrations. The concentrations for ellagic acid and kaempferol-3-*O*-rutinoside were 140.0, 70.0, 35.0, 18.0, 9.0, 4.5, and 2.3 μg/mL and 65.0, 33.0, 16.0, 8.0, 4.0, 2.0, and 1.0 μg/mL, respectively. Each concentration was analyzed thrice under the above chromatographic method, and a linear regression analysis was performed with the peak area of a chromatographic peak as the ordinate (y) and the concentration of components in the reference substance solution as the abscissa (x) in the linear range.

2.4.2. Precision test

The mixed standard solution was analyzed according to Section 2.3 with six replicates. The relative standard deviation (RSD) of peak areas was calculated to evaluate the precision of the instrument.

2.4.3. Repeatability test

Six repetitive sample solutions were prepared in accordance with the procedure described in Section "2.2″, and then measured according to the chromatographic conditions mentioned in Section "2.3″, followed by quantification of the contents of the two components to evaluate the repeatability of the method.

2.4.4. Recovery rate test of sample addition

The same batch of raspberries was taken, crushed, sieved, and accurately weighed in 6 parallel, and moderately spiked with the standard solution of two components, followed by the preparation of the sample solution in accordance with the method described under Section "2.2". To this, an appropriate amount of ellagic acid and kaempferol-3-*O*-rutinoside reference substance was added, respectively, and the recovery rate of the sample was measured according to the chromatographic conditions described under Section "2.3". The average recovery rate and RSD of six parallel sample solutions were calculated to evaluate the accuracy of the method. The average recovery rate was calculated by the following formula:

$$\text{average recovery rate} = \frac{M_{detection} - M_{contain}}{M_{add}} \quad (1)$$

where $M_{detection}$ was the content of ellagic acid or kaempferol-3-*O*-rutinoside in each parallel sample solution detected by HPLC. $M_{contain}$ was that a certain amount of raspberry contained the content of ellagic acid or kaempferol-3-*O*-rutinoside. M_{add} was the content of ellagic acid or kaempferol-3-*O*-rutinoside was added into the sample solution.

2.4.5. Stability test

The same sample solution and the mixed reference solution were placed at room temperature and measured at 0, 2, 4, 8, 16, and 24 h in accordance with the chromatographic conditions described under Section "2.4". The measurement was repeated 6 times, followed by the stability test.

2.5. Single-factor experiments

The single-factor experiments were conducted under 4 extraction conditions: ultrasonic time (A), ethanol concentration (B), ultrasonic temperature (C), and solid-liquid ratio (D).

2.5.1. Effect of ultrasonic time on the yield

We took 5.00 g of raspberry coarse powder in a solid–liquid ratio of 1:20 (g/mL), added 70 % ethanol, and subjected it to ultrasonication at 50 °C for different time points (10, 15, 20, 25, 30, 45, and 60 min) to determine the yield of two components in the raspberry extract in order to investigate the effect of ultrasonic time on the respective yields of ellagic acid and kaempferol-3-*O*-

rutinoside.

2.5.2. Effect of ethanol concentration on the yield

Another 5.00 g of raspberry coarse powder was taken in a solid–liquid ratio of 1: 20 (g/mL) and subjected to ultrasonication for 30 min at 50 °C with different concentrations of ethanol (50 %, 60 %, 70 %, 80 %, and 90 %). The yields of the two components in the raspberry extract were determined to investigate the influence of ethanol concentration on their yields.

2.5.3. Effect of ultrasonic temperature on the yield

Another 5.00 g of raspberry coarse powder was taken in a solid–liquid ratio of 1: 20 (g/mL) with 70 % ethanol and subjected to ultrasonication for 30 min at different temperatures of 30, 40, 50, 60, and 70 °C in order to determine the yield of the two components in the raspberry extract so as to investigate the effect of ultrasonic temperature on the yield of the two components.

2.5.4. Effect of solid–liquid ratio on the yield

Another 5.00 g of raspberry coarse powder was extracted with 70 % ethanol and subjected to ultrasonication at 50 °C. The solid—liquid ratio of 1: 10, 1: 20, 1: 30, 1: 40, and 1: 50 (g/mL) was selected to determine the yield of the two components in the raspberry extract in order to investigate the effect of the solid–liquid ratio on the yield of ellagic acid and kaempferol-3-*O*-rutinoside in raspberry.

2.6. Determination of the comprehensive score

The entropy weight method [11] is an objective weighting method based on the concept of information entropy. The lower the entropy value, the greater the dispersion of the index, and the more significant the impact of the index on the results. The entropy weight method can eliminate the overlap of information, reflect the utility value of the information entropy value of the index, and has high reliability and accuracy. In this paper, the weight of the ellagic acid yield and kaempferol-3-*O*-rutinoside yield obtained by the factorial experiment was calculated by using the entropy weight method. Next, linear weighting was performed to calculate their comprehensive scores with reference to Equation (2).

$$y = w_1 x_1 + w_2 x_2, \tag{2}$$

where, y is the comprehensive score, and x_1 and x_2 are the yield of ellagic acid and kaempferol-3-*O*-rutinoside, respectively. Similarly, w_1 and w_2 are the corresponding weights.

2.7. Multivariate variance analysis

Variance analysis of the results of the factorial test was performed to investigate any possible interaction among the factors, and an appropriate optimization model was selected according to the analysis results.

In the experiment on extracting effective components of TCM, the possible interaction between the experimental factors has a great influence on the experimental results, and the interaction is extremely important to determine the parameters in the optimization process model. Therefore, this study first conducted an analysis of variance (ANOVA) on the results of a factorial experiment to determine the relationship between the factors. Taking 81 groups of the experimental results of ellagic acid yield as indicators, four factors including ultrasonic temperature (°C), ultrasonic time (min), ethanol concentration (%), and the solid-liquid ratio (g/mL) were analyzed by four-way ANOVA, and the single effect, main effect, and interaction of different factors and different levels on the ellagic acid yield were analyzed.

Similarly, the single effect, main effect, and interaction of different factors and different levels on kaempferol-3-*O*-rutinoside yield and the comprehensive score were discussed.

2.8. ACO-BPNN optimization model

BPNN is composed of an input layer, several hidden layers, and an output layer, which offers the advantages of simplicity and less computation. However, at the beginning of training, the setting of network weights, thresholds, the number of hidden neurons, and other parameters in the system were random, which easily led to an increase in the training error or over-fitting. ACO is a swarm optimization search algorithm based on the principle of ants foraging, which simulates the positive feedback phenomenon of ants on pheromones in collective foraging and gradually approaches the optimal path. In this study, the experimental data were normalized to eliminate the influence of dimension and magnitude. Based on the BPNN theory, the weights of the neural network and the number of hidden neurons were optimized based on the global optimization function of ACO. Then, the ACO-BPNN mathematical models for the ellagic acid yield, kaempferol-3-*O*-rutinoside yield, and comprehensive score were established. Finally, their optimized extraction conditions were determined through ACO based on the proposed models.

2.9. Network pharmacological analysis

The target points of the two components were screened through the database of TCM Pharmacology Database and Analysis Platform (TCMSP, https://tcmspw.com, 2022/12/23), and ellagic acid and kaempferol-3-*O*-rutinoside were screened in the database

of SwissTargetPrediction (http://www.swisstarget prediction.ch, 2022/12/24) with a score >0.5. The duplicate genes are merged and deleted as the target of the main components of raspberry.

The target of raspberry was entered in the String database (https://www.string-db.org/, 2022/12/24), the protein species were set as "*Homo sapiens*", and the minimum interaction threshold to 0.7, followed by the analysis of the PPI network of protein interaction [12]. The analyzed data were imported into Cytoscape 3.9.0 software, the topology was studied, and the core genes were analyzed.

The Bioconductor software package in R language, the GO analysis, and the KEGG analysis of the main components of raspberry were conducted under the condition of $P \leq 0.05$, and the enrichment of its gene function and the signal pathway were obtained.

The network of "traditional Chinese medicine-ingredients-targets-pathways" was constructed by using the software Cytoscape 3.9.0, and the core genes were obtained via topological research.

2.10. Molecular docking verification

In order to predict the docking between the main components of raspberry and the core target, the core gene obtained via target enrichment analysis was selected for molecular docking with ellagic acid and kaempferol-3-*O*-rutinoside. The protein structure was downloaded from the PDB database, and the Autodock Tools software was applied to remove water and hydrotreat protein. The structure files of the two core components were downloaded through the Pubchem database (https://pubchem.ncbi.nl.nih.gov, 2023/1/12). The molecular docking software Auto Dock Vina was used for molecular docking. If the docking binding energy was <0, the ligand could spontaneously bind to the receptor. The docking results were plotted and displayed by PyMol 2.3.0 [13].

3. Results

3.1. HPLC analysis of ellagic acid and kaempferol-3-O-rutinoside

The HPLC fingerprints of Fructus Rubi extract and the standard substance are depicted in Fig. 2 (a) and (b). At 350 nm, ellagic acid and kaempferol-3-*O*-rutinoside were separated well, and the number of theoretical plates was >6000. The yields of ellagic acid and kaempferol-3-*O*-rutinoside were calculated according to their peak areas.

3.2. Method validation

In order to inspect the linearity of the method, seven different concentrations of the mixed stock standard solution were analyzed. The regression equation of ellagic acid obtained through the linear range test was shown as equation (1).

$$Y = 2.594 \times 10^4 X - 75.07,\ R^2 = 0.9997 \quad (3)$$

And the regression equation of kaempferol-3-*O*-rutinoside was shown as equation (2).

$$Y = 2.584 \times 10^4 X - 12.42,\ R^2 = 0.9998 \quad (4)$$

The mixed standard solution was analyzed six times to evaluate the precision of the instrument. The RSD of the peak areas of ellagic acid and kaempferol-3-*O*-rutinoside was 0.19 % and 0.21 %, respectively, which indicates that the precision of the instrument was good.

Six repeats of sample solutions were analyzed to evaluate the precision of the method. The RSD of the average contents of ellagic acid and kaempferol-3-*O*-rutinoside were 1.65 % and 1.87 %, respectively, which indicated good repeatability of the method.

The average recovery rates of ellagic acid and kaempferol-3-*O*-rutinoside were 99.85 % and 100.23 %, and the RSD was 1.22 % and 0.95 %, respectively. These results indicated that the accuracy of the method was good.

The RSD for peak areas of ellagic acid and kaempferol-3-*O*-rutinoside in standard solution at 0, 2, 4, 8, 16, and 24 h were 0.39 % and 0.34 %, respectively. That of ellagic acid and kaempferol-3-*O*-rutinoside in the sample solution was 0.41 % and 0.36 %, respectively. These results revealed that the sample solution and standard solution were stable within 24 h.

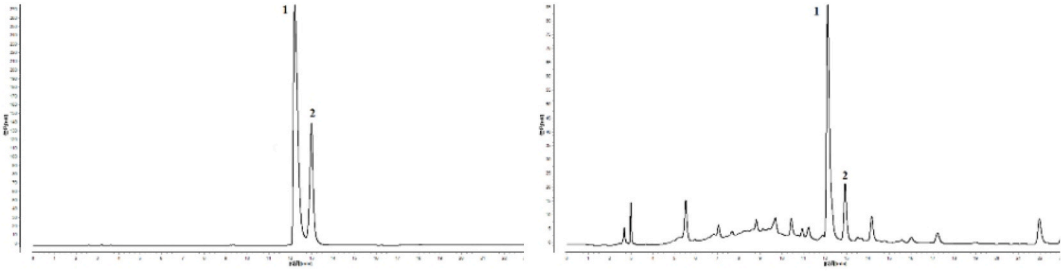

Fig. 2. HPLC chromatogram: (a) mixed reference; (b) extraction samples (1: Ellagic acid; 2: Kaempferol-3-*O*-rutinoside).

3.3. Single-factor experiments

Through the single-factor experiment of ellagic acid and kaempferol-3-*O*-rutinoside yields under 4 extraction conditions, the specific level range can be determined and the multi-factor factorial experiment was confirmed as 4-factors and 3-levels. The results of the single-factor test are shown in Fig. 3(a–d). The two components at different time points are displayed in Fig. 3 (a). The yields of both components reached the maximum at 30 min, whereas after 30 min, the yields decreased with an increase in ultrasonic time. Therefore, the optimum range of the ultrasonic time was set at 15–45 min.

The yields of the two components with different solvent concentrations are presented in Fig. 3 (b). When the ethanol concentration was 70 %, the yields of the two components became the maximum, whereas when the concentration was increased to more than 70 %, the yield decreased. Therefore, the optimum range of the ethanol concentration was set at 60%–80 %.

Fig. 3 (c) presents the yields of the two components at different ultrasonic temperatures. The yield of ellagic acid was the maximum when the ultrasonic temperature reached 50 °C, whereas when the temperature was higher than 50 °C, the ellagic acid yield decreased. The kaempferol-3-*O*-rutinoside yield exhibited an increase at 30–60 °C, and then a decrease at 60–70 °C. Therefore, the optimum range of the ultrasonic temperature was set at 40°C-60 °C.

Fig. 3 (d) illustrates the yields of the two components at different ratios of material to liquid. The ellagic acid yield reached the maximum when the solid-liquid ratio reached 1:20 g/mL. By contrast, when the ratio was more than 1:20 g/mL, the ellagic acid yield decreased. Meanwhile, the yield of kaempferol-3-*O*-rutinoside decreased at 1:10–1:20 g/mL, increased at 1:20–1:30 g/mL, and rapidly decreased at 1:30–1:50 g/mL. Therefore, the optimum range of the solid-liquid ratio was set at 1:10–1:30 g/mL.

3.4. Factorial experimental design with 4-factors and 3-levels

In the four-factor three-level factorial test, based on the abovementioned single-factor test results, ultrasonic temperature (°C), ultrasonic time (min), ethanol concentration (%), and solid-liquid ratio (g/mL) were selected as test factors, and the yields of ellagic acid and kaempferol-3-*O*-rutinoside in raspberry were used as test indicators. A total of 81 groups of experiments were performed.

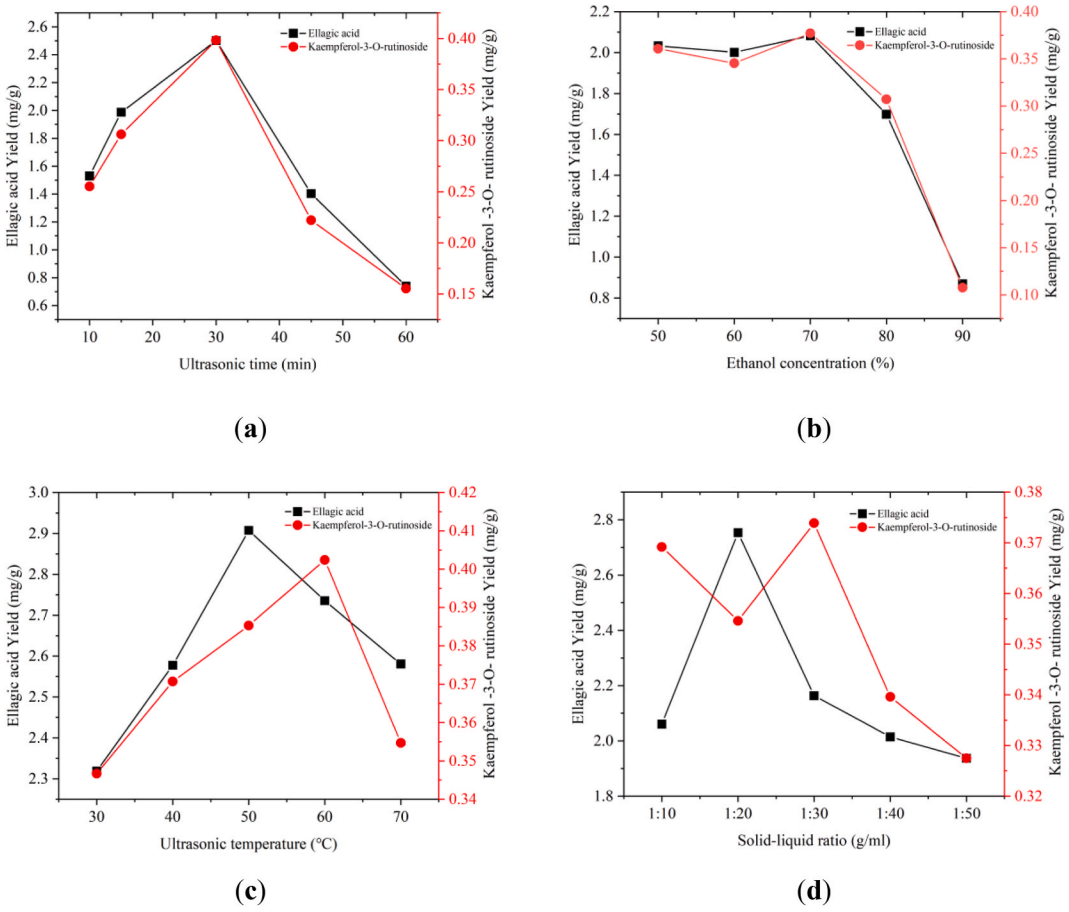

Fig. 3. The result of the single-factor test: (a) effect of ultrasonic time on yield; (b) effect of ethanol concentration on yield; (c) effect of ultrasonic temperature on yield; and (d) effect of solid-liquid ratio on yield.

Measurements were performed thrice for each group in parallel, and the average values were considered for subsequent analysis. The factors and levels are depicted in Table 1.

3.5. ANOVA of multivariate factorial test

3.5.1. Multivariate factorial test results

A, B, C, and D were simplified into the names of 4 factors. A represents the ultrasonic time (min), B is the ethanol concentration (%), C represents the ultrasonic temperature (°C), and D is the solid-liquid ratio (g/mL). Table 2 presents factorial test results.

The weights of ellagic acid and kaempferol-3-*O*-rutinoside yields determined using the entropy weight method were 0.5187 and 0.4813, respectively. The comprehensive score is shown in column 8 of Table 2.

3.5.2. Multivariate factorial test results

The four-way ANOVA of the ellagic acid and kaempferol-3-*O*-rutinoside yields and their comprehensive score was performed under the aforementioned different extraction conditions. Appendix Tables A1–A3 are the variance analysis tables of the ellagic acid yield, kaempferol-3-*O*-rutinoside yield, and comprehensive score, respectively. The smaller the P value is (more asterisks attached), the more significant the difference is.

Table A1–A3 show that the main effects and interactions of ultrasonic temperature (°C), ultrasonic time (min), ethanol concentration (%), and solid-liquid ratio (g/mL) on the ellagic acid yield, kaempferol-3-*O*-rutinoside yield, and comprehensive score are statistically significant. In addition to their individual effects, first-order interaction, second-order interaction, and other complex interactions were considered to exist among the 4 factors.

3.6. Determination of optimum process conditions

3.6.1. Determination of the BPNN structure

The BPNN had a 3-layer network structure, with 4 factors as the network inputs and a maximum number of training sessions was 500. We then considered the ellagic acid yield, kaempferol-3-*O*-rutinoside yield, and comprehensive score as network outputs. The number of individuals was 20, the learning rate of the ant colony was 0.85, the transfer parameter was 0.1, the pheromone volatilization coefficient was 0.1, and the learning rate of the BPNN was 0.1. Meanwhile, the activation function of the hidden layer was sigmoid and that of the output layer was linear. The hidden layer was set as 1 layer, and the neuron number in the hidden layer was selected. Seventy-three groups of test data were selected as the training set, and the average fitting error was calculated. The remaining 8 groups of data were considered a test set, and the average prediction error and the number of neurons were calculated. The curves of average fitting errors and average prediction errors are presented in Fig. 4(a–c).

In Fig. 4, the prediction error is minimized while the fitting error is kept as small as possible, and thus, the number of hidden neurons is selected as 3. Appendix Figure A1 presents the schematic diagram of the neural network structure. According to the aforementioned parameters, the initial ant colony matrix was randomly generated, and the BPNN was trained to calculate the optimal individual vector and fitness. Appendix Tables A4–A6 presents the weights of the trained neural networks. The relationship between the predicted and experimental yields of ellagic acid is shown in Fig. 5 (a), and the residual diagram is presented in Fig. 5 (b). The relationship between the predicted and experimental values of kaempferol-3-*O*-rutinoside yield and that between the predicted and experimental values of the comprehensive score are presented in Fig. 5 (c) and (e), respectively, and the residual diagrams are given in Fig. 5 (d) and (f), respectively.

Most points in the relationship diagram between the predicted and experimental values are evenly distributed on both sides of the straight line. Similarly, the points in the residual diagrams are evenly distributed on both sides, These observations indicate that ACO-BPNN has a good fitting effect on multivariate nonlinear functions.

3.6.2. Determination of the optimum extraction process and experimental verification

Based on the aforementioned ACO-BPNN models, using the global optimization function of ACO, the optimal production process combination was independently searched. Moreover, the optimal conditions and yields of individual and combined extraction of ellagic acid and kaempferol-3-*O*-rutinoside from raspberry are listed in Table 3.

We conducted the experiments according to the best extraction process. The ellagic acid yield was 2.7762 mg/g. The kaempferol-3-*O*-rutinoside yield was 0.5724 mg/g. When the two components were extracted together, the ellagic acid and kaempferol-3-*O*-rutinoside yields were 2.8961 and 0.4139 mg/g, respectively, and the comprehensive score was 1.7014. The aforementioned results confirm that the ACO-BPNN model is reliable.

Table 1
List of factorial experimental factors and their level.

level	factor			
	Ultrasonic time/min	Ethanol concentration/%	Ultrasonic temperature/°C	Material ratio/(g/mL)
1	15	60	40	1:10
2	30	70	50	1:20
3	45	80	60	1:30

Table 2
Four-factor and three-level factorial experimental design results table.

test number	Ultrasonic time (min)	Ethanol concentration (%)	Ultrasonic temperature (°C)	Solid-liquid ratio (mL/g)	Ellagic acid yield (mg/g)	Kaempferol-3-*O*-rutinoside yield (mg/g)	Comprehensive score
S1	15	60	40	1:10	0.9143 (±0.0)	0.2476	0.5934
S2	15	60	40	1:20	0.6927	0.1922	0.4518
S3	15	60	40	1:30	1.1009	0.2249	0.6793
S4	15	70	40	1:10	1.2322	0.2611	0.7648
S5	15	70	40	1:20	1.2427	0.2494	0.7646
S6	15	70	40	1:30	1.3778	0.2969	0.8575
S7	15	80	40	1:10	0.8252	0.1655	0.5077
S8	15	80	40	1:20	1.1047	0.1980	0.6683
S9	15	80	40	1:30	1.5213	0.2170	0.8935
S10	30	60	40	1:10	1.8678	0.4118	1.1670
S11	30	60	40	1:20	1.8257	0.3525	1.1166
S12	30	60	40	1:30	1.4056	0.3081	0.8774
S13	30	70	40	1:10	1.9042	0.3815	1.1713
S14	30	70	40	1:20	1.6434	0.3373	1.0148
S15	30	70	40	1:30	1.9033	0.3685	1.1646
S16	30	80	40	1:10	1.5390	0.3005	0.9429
S17	30	80	40	1:20	1.7819	0.3209	1.0787
S18	30	80	40	1:30	2.1215	0.3456	1.2668
S19	45	60	40	1:10	1.7132	0.3186	1.0420
S20	45	60	40	1:20	1.8253	0.3713	1.1255
S21	45	60	40	1:30	2.0990	0.3826	1.2729
S22	45	70	40	1:10	1.8616	0.3481	1.1331
S23	45	70	40	1:20	2.0343	0.3811	1.2386
S24	45	70	40	1:30	1.8913	0.3287	1.1392
S25	45	80	40	1:10	1.6924	0.2177	0.9826
S26	45	80	40	1:20	1.7458	0.2657	1.0335
S27	45	80	40	1:30	1.7889	0.2415	1.0441
S28	15	60	50	1:10	1.4445	0.3119	0.8993
S29	15	60	50	1:20	1.3492	0.3183	0.8530
S30	15	60	50	1:30	1.6899	0.3059	1.0238
S31	15	70	50	1:10	1.2865	0.3154	0.8191
S32	15	70	50	1:20	1.3911	0.3029	0.8674
S33	15	70	50	1:30	1.7421	0.3551	1.0746
S34	15	80	50	1:10	1.2219	0.2080	0.7339
S35	15	80	50	1:20	1.6041	0.3051	0.9789
S36	15	80	50	1:30	1.8023	0.2461	1.0533
S37	30	60	50	1:10	1.6136	0.2524	0.9584
S38	30	60	50	1:20	1.7856	0.3099	1.0754
S39	30	60	50	1:30	1.8002	0.3418	1.0983
S40	30	70	50	1:10	1.7759	0.3173	1.0739
S41	30	70	50	1:20	2.1113	0.3983	1.2868
S42	30	70	50	1:30	2.3636	0.4044	1.4206
S43	30	80	50	1:10	1.4334	0.2812	0.8788
S44	30	80	50	1:20	1.7643	0.3016	1.0603
S45	30	80	50	1:30	1.8661	0.3342	1.1288
S46	45	60	50	1:10	1.5075	0.3484	0.9496
S47	45	60	50	1:20	1.9127	0.3828	1.1764
S48	45	60	50	1:30	1.7366	0.3586	1.0734
S49	45	70	50	1:10	1.8210	0.3871	1.1309
S50	45	70	50	1:20	1.7854	0.3665	1.1025
S51	45	70	50	1:30	2.3936	0.4134	1.4405
S52	45	80	50	1:10	1.4748	0.1621	0.8430
S53	45	80	50	1:20	1.7946	0.2658	1.0588
S54	45	80	50	1:30	1.9806	0.3222	1.1824
S55	15	60	60	1:10	1.2533	0.2678	0.7790
S56	15	60	60	1:20	1.8040	0.3157	1.0877
S57	15	60	60	1:30	1.5750	0.2918	0.9574
S58	15	70	60	1:10	1.4646	0.2962	0.9022
S59	15	70	60	1:20	1.4354	0.2641	0.8716
S60	15	70	60	1:30	2.1743	0.3619	1.3020
S61	15	80	60	1:10	1.4255	0.2670	0.8679
S62	15	80	60	1:20	1.1982	0.2413	0.7376
S63	15	80	60	1:30	1.8717	0.2657	1.0987
S64	30	60	60	1:10	1.3716	0.3342	0.8723
S65	30	60	60	1:20	2.1075	0.3894	1.2806
S66	30	60	60	1:30	2.3313	0.3781	1.3912
S67	30	70	60	1:10	1.9399	0.4123	1.2047

(*continued on next page*)

Table 2 (*continued*)

test number	Ultrasonic time (min)	Ethanol concentration (%)	Ultrasonic temperature (°C)	Solid-liquid ratio (mL/g)	Ellagic acid yield (mg/g)	Kaempferol-3-*O*-rutinoside yield (mg/g)	Comprehensive score
S68	30	70	60	1:20	1.7231	0.3237	1.0496
S69	30	70	60	1:30	2.3775	0.3473	1.4004
S70	30	80	60	1:10	1.6356	0.2666	0.9767
S71	30	80	60	1:20	1.9931	0.2845	1.1707
S72	30	80	60	1:30	2.1735	0.3751	1.3079
S73	45	60	60	1:10	1.7043	0.3821	1.0680
S74	45	60	60	1:20	2.1104	0.3811	1.2781
S75	45	60	60	1:30	1.6640	0.3373	1.0254
S76	45	70	60	1:10	1.8003	0.3850	1.1191
S77	45	70	60	1:20	2.0096	0.3889	1.2295
S78	45	70	60	1:30	2.2648	0.4098	1.3720
S79	45	80	60	1:10	1.6501	0.4098	1.0531
S80	45	80	60	1:20	1.9745	0.2907	1.1641
S81	45	80	60	1:30	1.9102	0.2803	1.1257

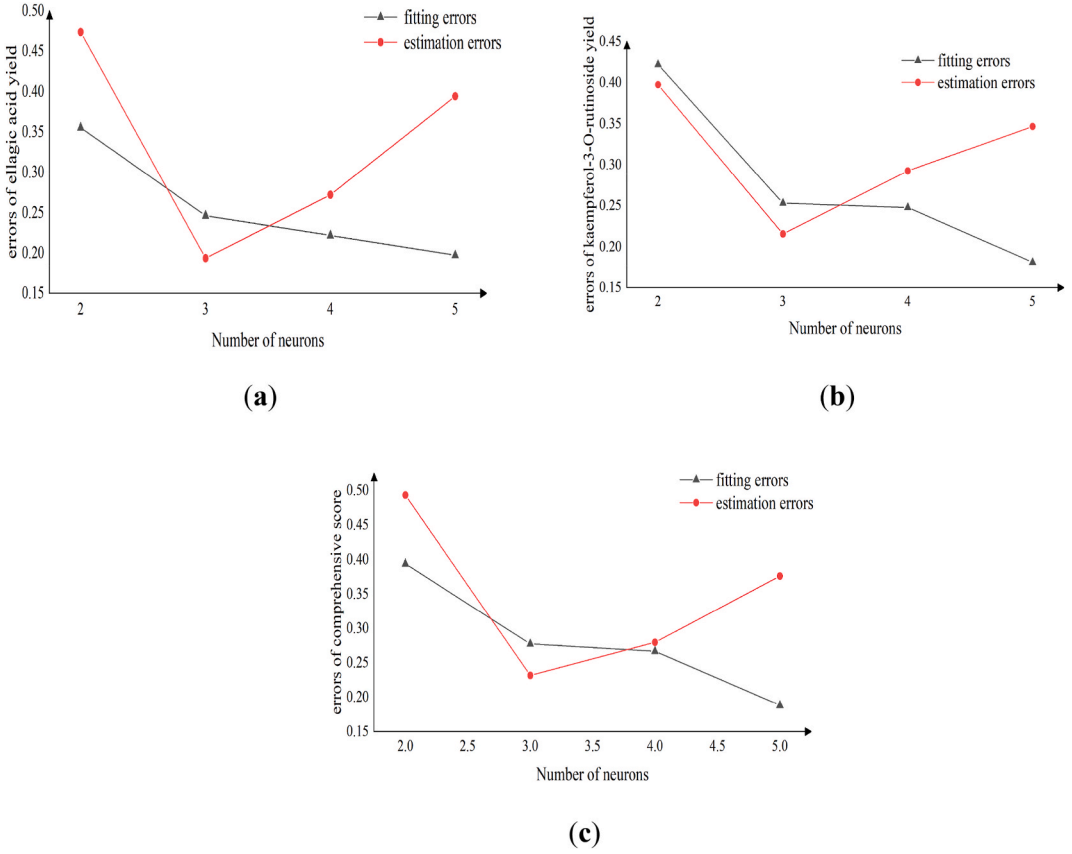

Fig. 4. Fitting error and prediction error diagram schemes: (a) yield of ellagic acid; (b) yield of kaempferol-3-*O*-rutinoside; (c) comprehensive score.

3.7. Network pharmacology

Sixty targets of ellagic acid and seven targets of kaempferol-3-*O*-rutinoside were screened from the TCMSP and SwissTarget databases. On combining the action targets of both components and deleting the duplicate values, 66 genes were obtained. These genes were input into the String database, and the protein-protein interaction (PPI) analysis was performed with the lowest interaction threshold of 0.7. The results were exported, and the PPI network was drawn in Cytoscape software, as shown in Fig. 6. Using the software, the genes ranked by degree value, and the top 5 genes were HSP90AA1, SRC, AKT1, EGFR and VEGFA.

Using the Bioconductor software package in R language, GO and KEGG analyses were performed with $P \leq 0.05$, and the results were displayed in the form of bar and bubble charts. GO annotation included the biological process (BP), molecular function (MF), and cellular component (CC), as shown in Fig. 7 (a) and (b). The results showed that the biological processes involved in the potential target

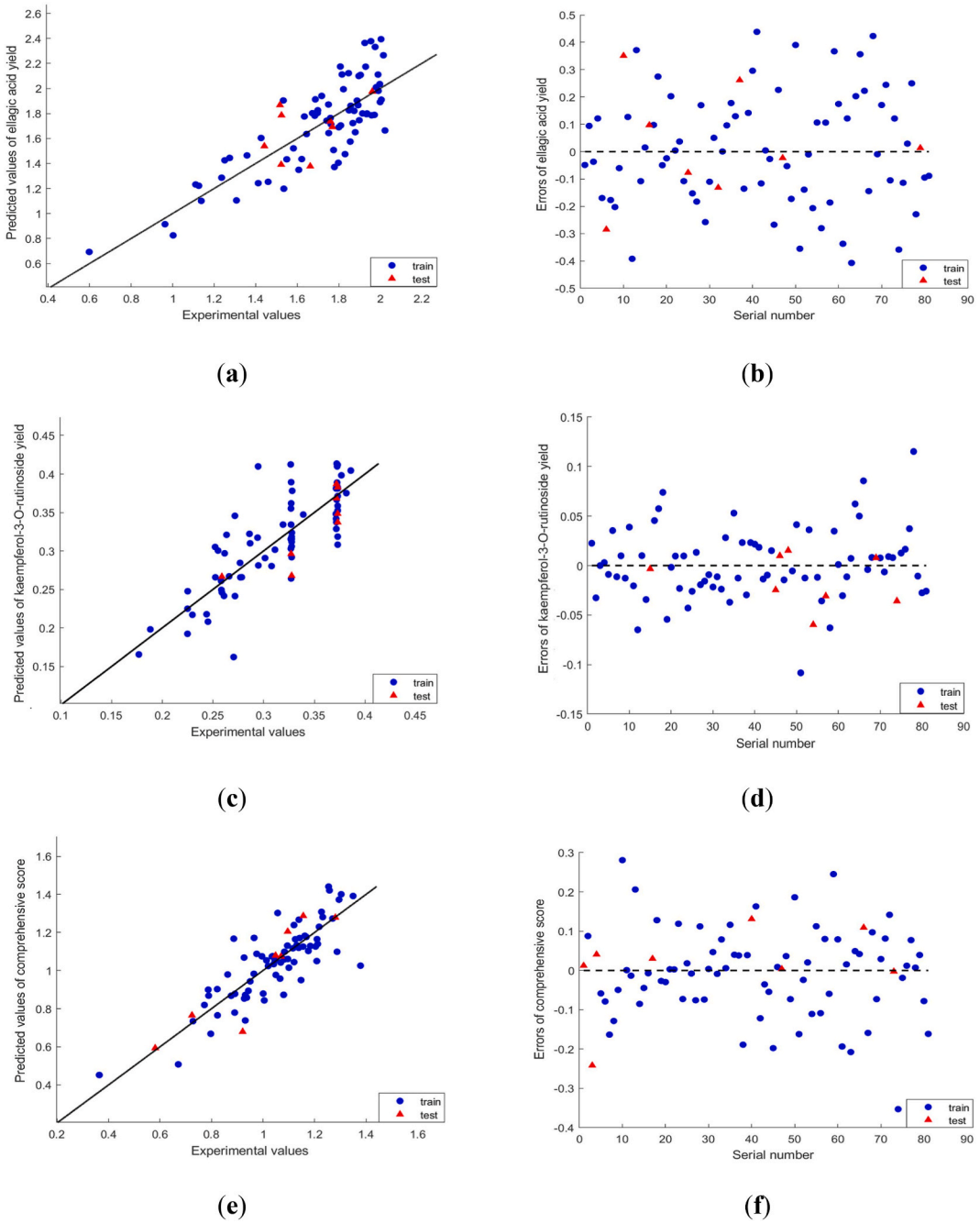

Fig. 5. Ellagic acid: (a) the relationship between the predicted and experimental values; (b) residual diagram. Kaempferol-3-*O*-rutinoside: (c) the relationship between predicted and experimental values; (d) residual diagram. Comprehensive score: (e) the relationship between predicted and experimental values; (f) residual diagram.

of raspberry were protein self-phosphorylation, carbon metabolism, and peptide-tyrosine modification. The cell components included the basal outer plasma membrane, membrane raft, and protein kinase complex. The molecular functions included protein tyrosine kinase, protein serine/threonine kinase, and carbonate dehydratase activities.

KEGG enrichment analysis revealed 112 pathways and the first 30 pathways were selected to draw bar and bubble charts, as shown in Fig. 7 (c) and (d). In Fig. 7 (d), the P value and dot size represent the significance of enrichment and the number of genes enriched in this pathway, respectively. The potential targets of raspberry were mainly concentrated in the PI3K-AKT, MAPK, Rap1, and Ras signal pathways. We selected 25 pathways rich in genes and drew a network diagram of "raspberry–components–target–pathways." The results are shown in Figure A3.

Table 3
Predicted values and actual value under optimal conditions optimized by ACO-BPNN.

	Ultrasonic time (min)	Ethanol concentration (%)	Ultrasonic temperature (°C)	Solid-liquid ratio (g/mL)	Yield (mg/g) or score	Actual Yield (mg/g) or score	Relative Error (%)
Ellagic acid	40.5	63	41	1:15	2.8433	2.7762	2.3599
Kaempferol-3-*O*-rutinoside	33	72	59	1:16	0.6184	0.5724	7.4386
Comprehensive score	37.5	60	59	1:29	1.7585	1.7014	3.2471

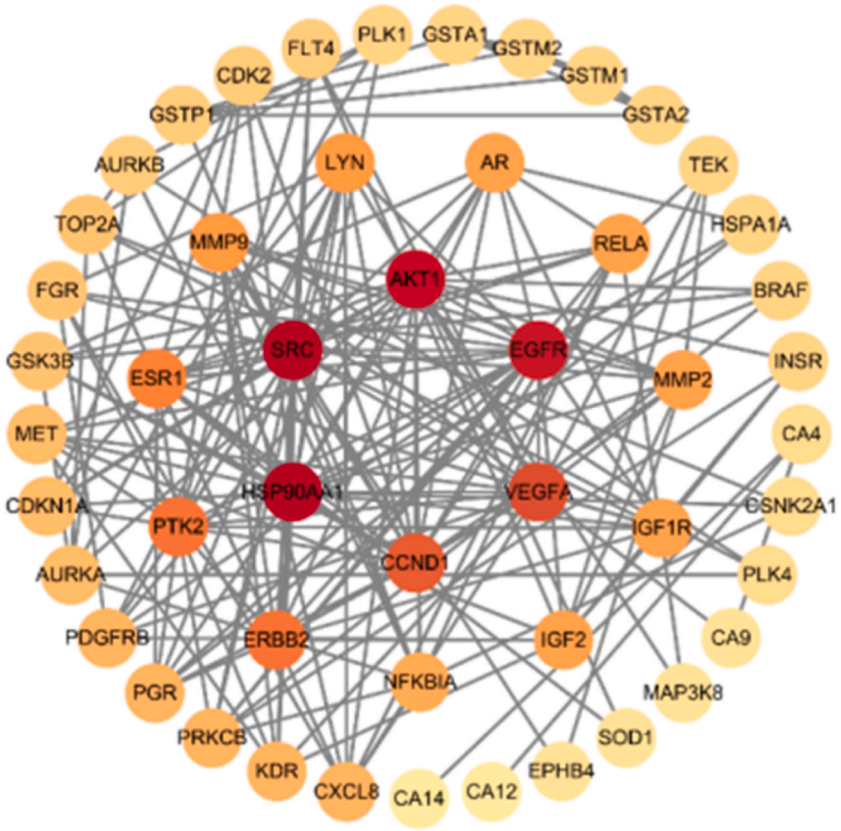

Fig. 6. Protein–protein interaction (PPI) analysis: a PPI network diagram of the sorting core targets of ellagic acid and kaempferol-3-*O*-rutinoside (the lowest interaction threshold of 0.7).

3.8. Molecular docking verification

To further predict the results of network pharmacology, the top five potential targets of raspberry were selected for molecular docking with ellagic acid and kaempferol-3-*O*-rutinoside. The binding energy of less than −5 kcal/mol indicated good binding activity, and the binding energy of less than −7 kcal/mol indicated strong binding activity (Refer to Table 4 for specific docking scores). PyMol was used to draw the docking mode of each core target and the two components, presenting the hydrogen bond formed by docking and marking the corresponding amino acid residues. The molecular docking mode diagram is presented in Appendix Figure A2.

4. Discussion

In this study, ellagic acid and kaempferol-3-*O*-rutinoside were simultaneously detected by the HPLC method. Then, the entropy weight method was used to calculate the comprehensive score of two components to transform multi-objective optimization into single-objective optimization. ACO-BPNN was used to optimize the extraction process of ellagic acid and kaempferol-3-*O*-rutinoside. Finally, network pharmacology and molecular docking were applied to find the potential therapeutic targets of ellagic acid and kaempferol-3-*O*-rutinoside for further pharmacological research.

The extraction yield of TCM is influenced by multi-factors including extraction time, solvent concentration, extraction temperature,

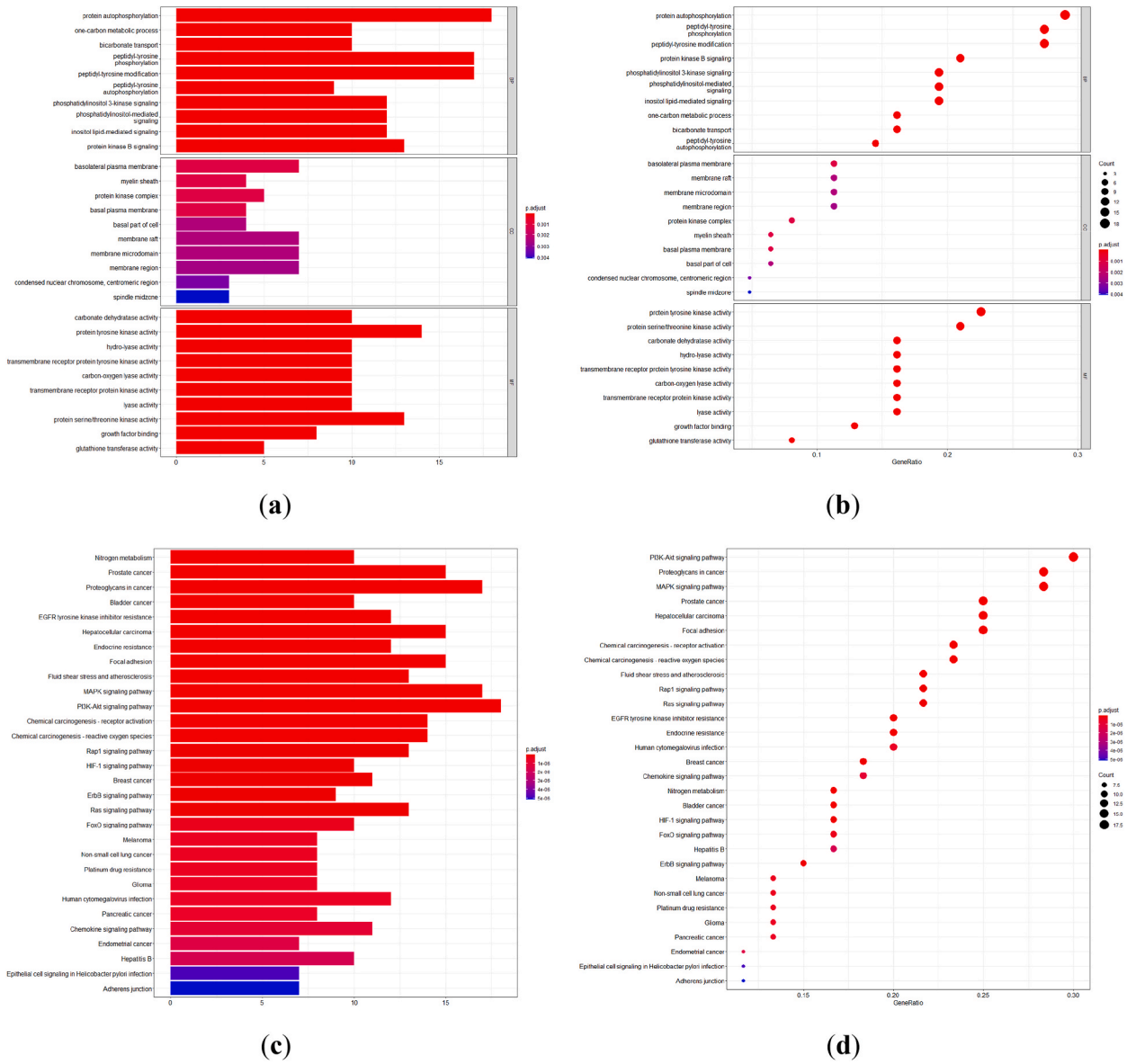

Fig. 7. GO enrichment analysis of raspberry including BP, MF, and CC: (a) bar chart (b) bubble chart (GO analyses were performed with $P \leq 0.05$) (BP: biological process) (MF: molecular function) (CC: cellular component). KEGG enrichment analysis of raspberry: (a) bar chart and (b) Bubble chart.

Table 4
Docking scores of ellagic acid and kaempferol-3-*O*-rutinoside and five core target molecules.

Genes	Ellagic acid binding energy (kcal/mol)	Kaempferol-3-*O*-rutinoside binding energy (kcal/mol)
HSP90AA1	−7.1	−8.3
SRC	−3.5	−5.1
AKT1	−3.9	−4.5
EGFR	−6.6	−9.9
VEGFA	−6.7	−5.6

solid-liquid ratio, and grain size. In this study, single-factor experiments (Fig. 3) showed that the yields of ellagic acid and kaempferol-3-*O*-rutinoside were significantly affected by ultrasonic time, ethanol concentration, ultrasonic temperature, and solid-liquid ratio. Meanwhile, there was an interaction between factors. Thus, the relationship between extraction conditions and yield of components was intricate. To ensure the accuracy of optimal results, this study adopted the factorial test (Table 2), matched all levels of the 4

factors, and repeated the factorial test in parallel, 3 times. Then, the multi-factor ANOVA was used to test the relationship between the factors. The ANOVA results (Table A1-A3) revealed that the linear coefficient and interactive coefficient significantly affected the yield of the effective components as well as had complex interactions among them. Therefore, the orthogonal experimental design and response surface experimental design are unsuitable for this experiment.

Due to the high-order nonlinear interaction between the factors, the linear regression model and low-order nonlinear model were not applicable. Therefore, adopting a machine learning model that can describe complex nonlinear relations is a feasible and reliable choice for us [14]. A neural network is composed of numerous interconnected neurons, which can fully approximate any nonlinear function in theory [15]. It has strong adaptability, learning ability, and nonlinear mapping ability. The number of hidden layer neurons affects the prediction and generalization capacity of the neural network. If hidden layer neurons are too few or too many, the model would be underfitting or overfitting, respectively. As shown in Fig. 4, when the number of hidden neurons was 3, the value of fitting errors and estimation errors were minimum. Thus, a neural network with 3 hidden-layer neurons was applied for further research. Based on this understanding, the ACO-BPNN model was established to optimize the individual and combined extraction process of effective components of raspberry, namely ellagic acid and kaempferol-3-*O*-rutinoside. As shown in Fig. 5, the experimental values of the yield of ellagic acid and kaempferol-3-*O*-rutinoside, and the comprehensive were very close to that of predicated value, which indicated that the established ACO-BPNN model was successfully applied for the optimization of extraction process of raspberry. The optimal extraction conditions optimized by ACO-BPNN were shown in Table 4. Although the actual values under the optimal extraction conditions were slightly lower than the predicted value, the actual value was larger than that in Table 2. The results of ACO-BPNN model optimization and experimental verification revealed significant differences in the best technological conditions for extracting different effective components. Therefore, in clinical applications, different extraction processes should be selected according to the actual situation.

Network pharmacology and molecular docking were applied to find the potential therapeutic targets of ellagic acid and kaempferol-3-*O*-rutinoside for further pharmacological study. In total, 66 key targets were screened out from the TCMSP database, and PPI analysis revealed that HSP90AA1, SRC, AKT1, EGFR, and VEGFA might be the core targets. GO function enrichment analysis (Fig. 7) showed that the targets ellagic acid and kaempferol-3-*O*-rutinoside might be closely related to protein self-phosphorylation, carbon metabolism, and peptide-tyrosine modification; basal outer plasma membrane, membrane raft, and protein kinase complex; protein tyrosine kinase, protein serine/threonine kinase, and carbonate dehydratase activities. KEGG function enrichment analysis (Fig. 7) showed that the potential targets of raspberry were mainly concentrated in the PI3K-AKT, MAPK, Rap1, and Ras signal pathways. Then, the two components further regulate PI3K-AKT, MAPK, Rap1, Ras, and other signal pathways involved in lung cancer, liver cancer, and other tumor diseases and thus can be used for the treatment of these conditions [16–19].

With molecular docking technology, the binding ability of the active raspberry components ellagic acid and kaempferol-3-*O*-rutinoside to the key targets HSP90AA1, SRC, AKT1, EGFR, and VEGFA can be easily verified. The results (Table 4) showed binding sites present between the active components and key targets, and the lowest binding energy ranged from −9.9 to −3.5 kJ/mol. The results revealed that the active raspberry components, ellagic acid and kaempferol-3-*O*-rutinoside, had the characteristics of multi-targets, multi-channels, and multi-mechanisms. These results act as a reference for the in-depth research of ellagic acid and kaempferol-3-*O*-rutinoside in cancer treatment.

5. Conclusions

In this study, variance analysis of the results of the factorial test was performed to verify that there were complex interactions among four factors in the extraction experiment of active components of raspberry, namely ellagic acid and kaempferol-3-*o*-rutinoside. Based on this, the ant colony algorithm and neural network model are combined to describe the highly nonlinear relationship between extraction conditions, and the best conditions for single component extraction and joint extraction are predicted. For the comprehensive score of joint extraction, the weights of ellagic acid and kaempferol-3-*O*-rutinoside were 0.5187 and 0.4813, respectively. The optimal condition was as follows: ultrasonic time 37.5 min, ethanol concentration 60 %, ultrasonic temperature 59 °C, and solid-liquid ratio 1:29 g/mL. Under the optimal condition, the comprehensive score was 1.7014. The relative error between the experimental and predicted values conducted on the same conditions is only 3.2471 %, which confirms the reliability of the ACO-BPNN model.

Although the ACO-BPNN model established in this study was successfully applied to optimize the optimal extraction conditions of ellagic acid and kaempferol-3-*O*-rutinoside, the relationship between extraction and yield was still unknown due to the inexplicability of the neural network. Additionally, in order to further study the pharmacological effects of raspberry, the network pharmacology and molecular docking of its active components were carried out.

Network pharmacology showed the core targets of ellagic acid and kaempferol-3-*O*-rutinoside were HSP90AA1, SRC, AKT1, EGFR, and VEGFA. The targets of ellagic acid and kaempferol-3-*O*-rutinoside were mainly concentrated in the PI3K-AKT, MAPK, Rap1, and Ras signal pathways. Molecular docking revealed that the combination of ellagic acid and HSP90AA1 was best, and the combination of kaempferol-3-*O*-rutinoside and EGFR was best.

Network pharmacology and molecular docking revealed the therapeutic target and mechanism of action of ellagic acid and kaempferol-3-*O*-rutinoside. Nevertheless, these results were just an inference without experimental verification. It needs more in-depth supplementary experiments at the cellular level, and its current role is more to act as a reference for further clinical research.

All in all, raspberry has a wide range of medicinal value and utilization prospects. Using an intelligent algorithm to optimize the extraction process of raspberry can effectively improve the accuracy of its pharmacology and pharmacodynamics, which has a vital reference value for quality control and clinical medication of raspberry.

Funding statement

This work was supported by the grant from the Major bidding project of Zhejiang Chinese Medical University [Grant No. ZB222006] and Educational Science Planning Project of Zhejiang Province [Grant No. 2022SCG428].

Data availability statement

Data associated with our study has not been deposited into a publicly available repository. All data are presented in this paper.

Ethics statement

Review and/or approval by an ethics committee was not needed for this study because animal experiments and clinical studies were not involved.

Informed consent was not required for this study because clinical studies were not involved.

CRediT authorship contribution statement

Xuming Chen: Writing – original draft, Visualization, Software, Methodology, Investigation, Formal analysis, Data curation. **Xiaochun Shi:** Validation, Investigation, Data curation. **Xiaohong Li:** Writing – review & editing, Supervision, Resources, Project administration, Funding acquisition, Conceptualization.

Declaration of competing interest

The authors declare the following financial interests/personal relationships which may be considered as potential competing interests:Xiaohong Li reports financial support was provided by the Major bidding project of Zhejiang Chinese Medical University. Xiaohong Li reports financial support was provided by the Educational Science Planning Project of Zhejiang Province.

Appendix A

Table A1
Variance analysis table of ellagic acid yield.

Source	degree of freedom	SS	MS	F	P
Sum	242	38.416			0.000***
A	2	2.240	1.12	270.393	0.000***
B	2	2.022	1.011	244.050	0.000***
C	2	10.031	5.016	1210.996	0.000***
D	2	6.802	3.401	244.050	0.000***
AB	4	0.496	0.124	29.964	0.000***
AC	4	0.520	0.130	31.383	0.000***
AD	4	1.332	0.333	80.405	0.000***
BC	4	2.574	0.644	155.381	0.000***
BD	4	1.305	0.326	78.796	0.000***
CD	4	1.019	0.255	61.496	0.000***
ABC	8	2.096	0.262	63.265	0.000***
ABD	8	1.470	0.184	44.380	0.000***
ACD	8	1.156	0.144	34.885	0.000***
BCD	8	1.423	0.178	42.948	0.000***
ABCD	16	3.258	0.204	49.172	0.000***
Error	162	0.671	0.004		

Note: ***$P < 0.001$ indicates a significant difference. (When the p value of variance analysis is less than 0.001, it indicates a significant difference, with three asterisks often marked in the upper right corner of it).

Table A2
Variance analysis table of kaempferol-3-*O*-rutinoside yield.

Source	degree of freedom	SS	MS	F	P
Sum	242	1.244			0.000***
A	2	0.218	0.109	520.152	0.000***
B	2	0.045	0.023	107.372	0.000***
C	2	0.231	0.115	549.839	0.000***
D	2	0.037	0.019	88.856	0.000***
AB	4	0.032	0.008	38.102	0.000***

(*continued on next page*)

Table A2 (*continued*)

Source	degree of freedom	SS	MS	F	P
AC	4	0.064	0.016	76.678	0.000***
AD	4	0.026	0.006	30.775	0.000***
BC	4	0.119	0.030	142.167	0.000***
BD	4	0.066	0.016	78.528	0.000***
CD	4	0.017	0.004	20.141	0.000***
ABC	8	2.096	0.010	47.353	0.000***
ABD	8	1.47	0.004	19.735	0.000***
ACD	8	1.156	0.004	18.749	0.000***
BCD	8	1.423	0.008	36.474	0.000***
ABCD	16	3.258	0.009	44.36	0.000***
Error	162	0.671	0		

Note: ***P $<$ 0.001 indicates a significant difference.

Table A3
Variance analysis table of comprehensive score.

Source	degree of freedom	SS	MS	F	P
Sum	242	13.289			0.000***
A	2	0.854	0.427	323.645	0.000***
B	2	0.705	0.352	267.293	0.000***
C	2	3.509	1.755	1330.56	0.000***
D	2	2.088	1.044	791.592	0.000***
AB	4	0.192	0.048	36.32	0.000***
AC	4	0.227	0.057	42.993	0.000***
AD	4	0.454	0.114	86.115	0.000***
BC	4	0.931	0.233	176.423	0.000***
BD	4	0.475	0.119	90.04	0.000***
CD	4	0.331	0.083	62.679	0.000***
ABC	8	0.743	0.093	70.388	0.000***
ABD	8	0.5	0.062	47.35	0.000***
ACD	8	0.378	0.047	35.815	0.000***
BCD	8	0.523	0.065	49.608	0.000***
ABCD	16	1.168	0.073	55.351	0.000***
Error	162	0.214	0.001		

Note: ***P $<$ 0.001 indicates a significant difference.

Table A4
Network weight table of ellagic acid.

Source	W1	W2	W3	W4	B1
Input layer - Hidden layer	−0.566612 601	−2.038548 708	0.498573 184	−1.393586 755	−0.123518 728
	−18.01727 295	9.748867 989	−31.9825 4776	−5.97706 6994	5.334216 595
	−19.21813 202	11.18453 026	−29.5112 5908	−4.53166 8186	2.771512 985
Hidden layer - Output layer	−4.450110 435	−7.364946 365	7.099225 998		0.922455 37

Table A5
Network weight table of Kaempferol-3-*O*-rutinoside.

Source	W1	W2	W3	W4	B1
Input layer - Hidden layer	−20.97844 124	31.13389 206	−1.00356 6861	0.005726 687	−1.20501 709
	19.80985 451	−42.16384 506	−4.86738 2526	−4.796941 757	12.15557 384
	−0.781405 151	0.323074 43	9.79118 824	−0.247645 602	−10.2921 1903
Hidden layer - Output layer	−6.273861 885	−6.915163 517	−4.00409 6031		7.122010 231

Table A6
Network weight table of comprehensive score.

Source	W1	W2	W3	W4	B1
Input layer - Hidden layer	−1.033065 677	−4.343650 818	0.272309 512	−0.88476 8665	−1.30532 8131

(*continued on next page*)

Table A6 (*continued*)

Source	W1	W2	W3	W4	B1
	3.904290	8.653322	20.93261	16.01411	−6.92094
	676	22	909	438	5644
	−12.88797	−22.81251	−33.33494	−34.92029	14.27882
	188	144	949	19	29
Hidden layer - Output layer	−10.11578	7.212664	7.191535		−6.640255
	369	604	473		451

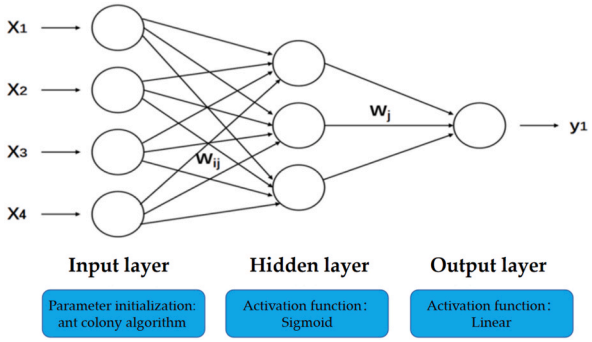

Fig. A1. Schematic diagram of neural network structure.

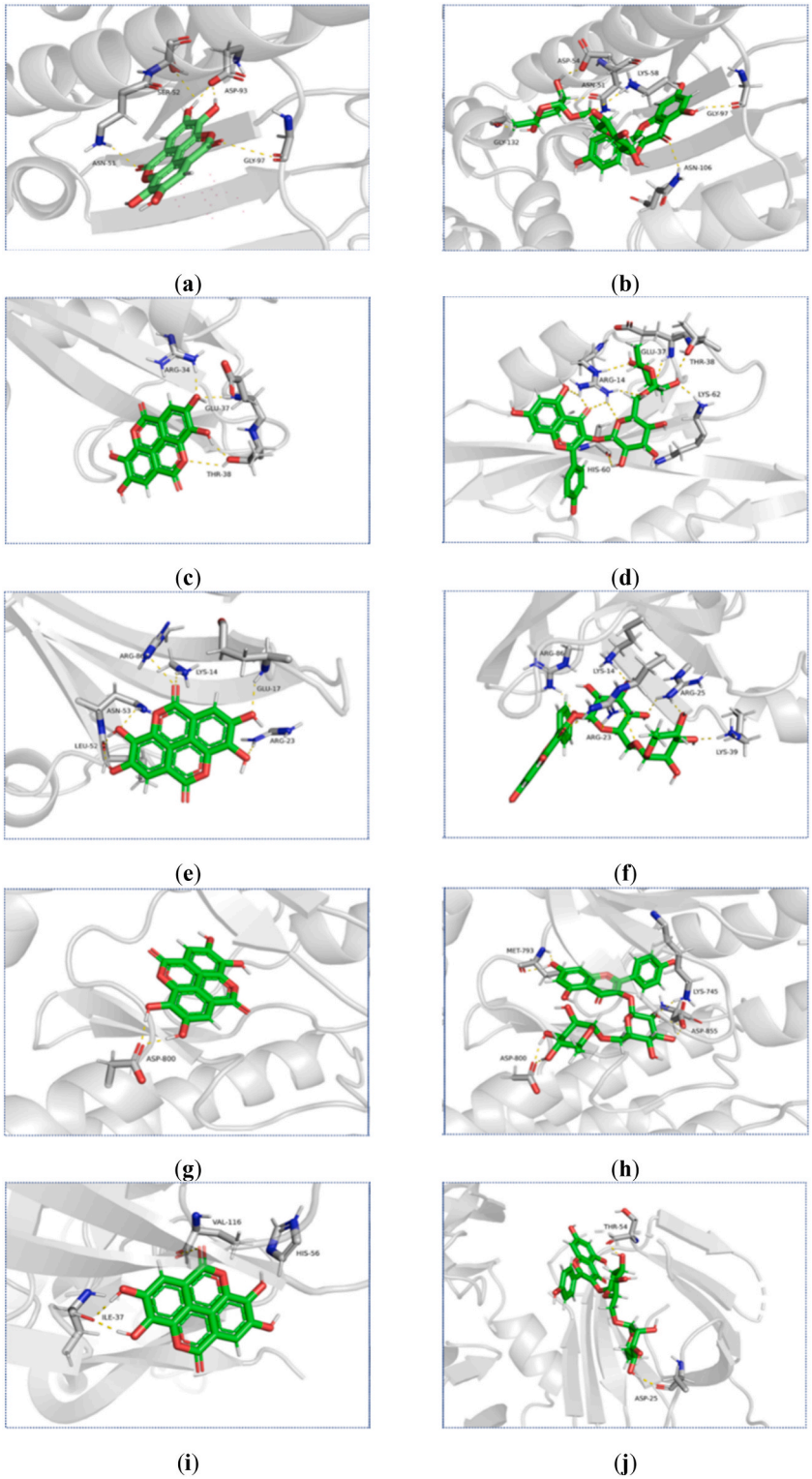

Fig. A2. Schematic diagram of docking between main components of raspberry and core targets: (a) HSP90AAI-Ellagic acid (b) HSP90AAI-Kaempferol-3-*O*-rutinoside (c) SRC-Ellagic acid (d) SRC-Kaempferol-3-*O*-rutinoside (e) AKT1-Ellagic acid (f) AKT1-Kaempferol-3-*O*-rutinoside (g) EGFR-Ellagic acid (h) EGFR-Kaempferol-3-*O*-rutinoside (i) VEGFA-Ellagic acid (j) VEGFA-Kaempferol-3-*O*-rutinoside.

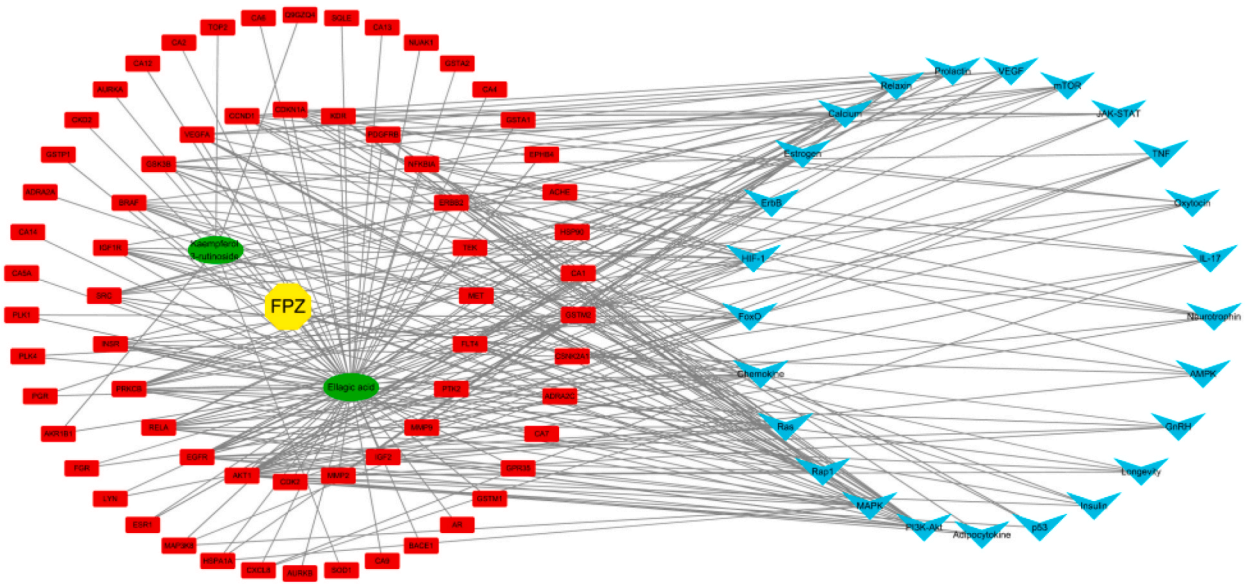

Fig. A3. "Raspberry-composition-target-pathway" network diagram (we only selected 25 pathways rich in genes to draw).

References

[1] Y. Chen, Y. Wang, L. Xu, Y. Jia, Z. Xue, M. Zhang, et al., Ultrasound-assisted modified pectin from unripe fruit pomace of raspberry (Rubus chingii Hu): structural characterization and antioxidant activities, LWT–Food Sci. Technol. 134 (2020), 110007, https://doi.org/10.1016/j.sc.2010.00372.

[2] D. Cheng, J. Li, B. Zhou, P. Zheng, Research progress on chemical constituents and pharmacological effects of raspberry, Zhong Yao Cai 35 (11) (2012) 1873–1876, https://doi.org/10.13863/j.issn1001-4454.2012.11.043.

[3] B. He, L. Dai, L. Jin, Y. Liu, X. Li, M. Luo, et al., Bioactive components, pharmacological effects, and drug development of traditional herbal medicine Rubus chingii Hu (Fu-Pen-Zi), Front. Nutr. 9 (2023), https://doi.org/10.3389/FNUT.2022.1052504, 1052504-1052504.

[4] X. Zhou, D. Cao, Raspberry, a precious medicinal and edible fruit in forest, South China Agric. 8 (9) (2014) 38+154, https://doi.org/10.19415/j.cnki.1673.

[5] Y. Ji, X. Bao, Y. Shan, S. Yang, L. Zhang, S. Hou, et al., Protective effect of raspberry extract on ConA-induced acute liver injuryin mice, China J. Chin. Mater. Med. 44 (4) (2019) 774–780, https://doi.org/10.19540/j.cnki.cjcmm.20181101.005.

[6] X. Zhang, Y. Liao, Z. Yang, Z. Chen, C. Hu, Effect of fupenzi (raspberry) with or without salt processing on kidney improvement in rats with kidney yang deficiency and polyuria, Chin. Arch. Tradit. Chin. Med. 39 (2) (2021) 140–142+276, https://doi.org/10.13193/j.issn.1673-7717.2021.02.036.

[7] Y. Qu, W. Wang, J. Cao, Y. Wang, M. Liu, C. Shen, P. Song, Research progress on preparation and application of ellagic acid, Food Nutr. China 28 (6) (2022) 39–45, https://doi.org/10.19870/j.cnki.11-3716/ts.2022.06.003.

[8] L.S. Sajan, A. Ghulam, S. Hina, S. A S, C.M. Iqbal, Z B. F. Synthesis and antiglycation activity of kaempferol-3-O-rutinoside (nicotiflorin), Med. Chem. 8 (3) (2012) 415–420, https://doi.org/10.2174/1573406411208030415.

[9] Y. Yang, P. Yuan, A. Feng, Mechanisms of Morindae Officinalis Radix in treatment of rheumatoid arthritis based on network pharmacology and molecular docking, Zhong Cao Yao 53 (5) (2022) 1463–1470, https://doi.org/10.7501/j.issn.0253-2670.2022.05.022.

[10] R. Xu, R. Xue, X. Mei, J. Gong, Q. Zhang, X. Zhao, et al., Q-Markers prediction of Zhishi Xiebai Guizhi Decoction based on fingerprint and network pharmacology, Zhong Cao Yao 53 (2) (2022) 372–381, https://doi.org/10.7501/j.issn.0253-2670.2022.02.007.

[11] G. Chen, W. Jin, S. Xu, L. Zhang, Y. Wang, Y. He, Decocting process optimization of Astragali Radix-Carthami Flos drug pair based on spherical symmetry design and genetic neural network, Zhong Cao Yao 52 (8) (2021) 2257–2266, https://doi.org/10.7501/j.issn.0253-2670.2021.08.008.

[12] Z. Lin, W. Fan, X. Yu, J. Liu, P. Liu, Research into the mechanism of intervention of SanQi in endometriosis based on network pharmacology and molecular docking technology, Medicine 101 (37) (2022), e30021, https://doi.org/10.1097/MD.0000000000030021. Article.

[13] L. Wu, Y. Liu, Y. Qin, L. Wang, Z. Wu, HPLC-ESI-qTOF-MS/MS characterization, antioxidant activities and inhibitory ability of digestive enzymes with molecular docking analysis of various parts of raspberry (Rubus ideaus L.), Antioxidants. 8 (8) (2019) 274, https://doi.org/10.3390/antiox8080274.

[14] L. Yu, H. Wan, Y. He, H. Zhou, W. Jin, C. Li, et al., Optimization of the extraction process of hydroxy safflower yellow A in Carthamus tinctorius based on two analytical methods, Zhong Yao Cai 41 (11) (2018) 2627–2631, https://doi.org/10.13863/j.issn1001-4454.2018.11.030.

[15] P. Huang, W. Jin, H. Wan, C. Li, J. Chen, X. Lou, et al., Optimization of microwave extraction conditions of astragalus saponins by genetic neural network and genetic algorithm, Zhong Cao Yao 50 (16) (2019) 3815–3823, https://doi.org/10.7501/j.issn.0253-2670.2019.16.012.

[16] Y. Wang, F. Ren, B. Li, Z. Song, P. Chen, L. Ouyang, Ellagic acid exerts antitumor effects via the PI3K signaling pathway in endometrial cancer, J. Cancer 10 (15) (2019) 3303–3314, https://doi.org/10.7150/jca.29738.

[17] Z. Deng, G. Huang, X. Qin, Z. Huang, Research progress of correlations between P38 MAPK signaling pathway and liver diseases, Med. Recapitulate 26 (22) (2020) 4395–4403, 10.3969/j.issn.1006-2084.2020. 22.006.

[18] H. Zhang, L. Zhao, H. Li, H. Xu, W. Chen, L. Tao, Research progress on the anticarcinogenic actions and mechanisms of ellagic acid, Cancer Biol. Med. 11 (2) (2014) 92–100, https://doi.org/10.7497/j.issn.2095-3941.2014.02.004.

[19] J. Wang, X. Fang, L. Ge, F. Cao, L. Zhao, Z. Wang, et al., Antitumor, antioxidant and anti-inflammatory activities of kaempferol and its corresponding glycosides and the enzymatic preparation of kaempferol, PLoS One 13 (5) (2018), e0197563, https://doi.org/10.1371/journal.pone.0197563.